The Institute of Space and Astronautical Science
Report SP No.14, December 2000

The Subaru Telescope and the HII/L2 Mission (SPICA)

By

Masahiko HAYASHI*

(November 1, 2000)

Abstract: An overview is given of the Subaru telescope, an 8.2 m diameter optical-infrared telescope atop Mauna Kea, together with representative first light images which proved the high performance of the telescope. Expectation for Japan's HII/L2 mission SPICA to be launched at the end of this decade is described.

1. SUBARU TELESCOPE

The Subaru telescope is an 8.2 m diameter optical-infrared telescope located at the summit of Mauna Kea, Hawaii (Figures 1 & 2). The telescope project was funded in 1991 for 9 years of construction, after its research and development phase in the 1980's. Its open use observations will begin in December, 2000.

An overview of the Subaru telescope is given in Table 1. The Subaru project is entirely funded by the Japanese government (Ministry of Education, Science, Sports, and Culture). "Subaru" is named after the old Japanese word for the young star cluster Pleiades.

The Subaru telescope utilizes the latest technologies to achieve the maximum performance of ground based telescopes located at the best sites in the world. The monolithic, thin meniscus primary mirror is made of ULE (ultra low expansion) glass and is supported by 261 actuators. Each actuator is sensitive to the force variation of 1 g to keep the surface accuracy of ~0.1 μm or better during observations while supporting more than ~100 kg of its share of the total mirror weight. Its cylindrical enclosure was designed to prevent ground-surface turbulence from being blown up over the telescope beam. The telescope main structure was placed in a narrow, air-conditioned channel where ventilators allow efficient flushing of turbulent air. There are 4 foci available for observing instruments: 1 Cassegrain, 2 Nasmyth, and 1 prime. At the base facility of the Subaru telescope located in Hilo, Hawaii, we have hardware and software simulators for the telescope and observing instruments as well as computers for data reduction.

We have been fabricating 7 observatory instruments and a near-infrared adaptive optics system for the Subaru telescope (Table 2). We started commissioning and test observations of

---

* Subaru Telescope, 650 North A‘ohōkū Place, Hilo, HI 96720, USA; masa@subaru.naoj.org

Fig. 1: Aerial view of the Subaru telescope in its enclosure.

these instruments one after another from late 1999. Among the instruments IRCS (without AO) and Suprime-Cam will be used for the initial open use. IRCS has a near-infrared echelle spectroscopic capability which enables us to obtain an entire K-band spectrum with a resolution of 20,000 in only 2 echelle configurations. Equipped with 10 pieces of 2 K×4 K CCDs, Suprime-Cam (Subaru prime focus camera) covers most of the $30'$ field of view at the prime focus and will be a workhorse instrument to survey faint, unknown objects in the Universe.

2. FIRST LIGHT OBSERVATIONS

After initial engineering adjustments started in late December, 1998, we carried out test observations of astronomical targets in January, 1999, in order to check the basic performance of the telescope at the very beginning phase.

The seeing size of $0\farcs3$ – $0\farcs5$ was frequently observed in the near-infrared, proving the high imaging capability of the Subaru telescope under the excellent atmospheric stability at the Mauna Kea summit. We obtained the best natural seeing of $0\farcs2$ in the near-infrared in May 1999. This means that the primary mirror surface was satisfactorily controlled with the actuators. In this section I present several first light images which best demonstrate the capabilities of the Subaru telescope.

2.1 New Infrared Image of Orion Nebula

Figure 3 shows an image of the Orion nebula covering a $5' \times 5'$ area centered on the Trapezium cluster seen at the center (Kaifu et al. 2000). The image was obtained with the near-infrared

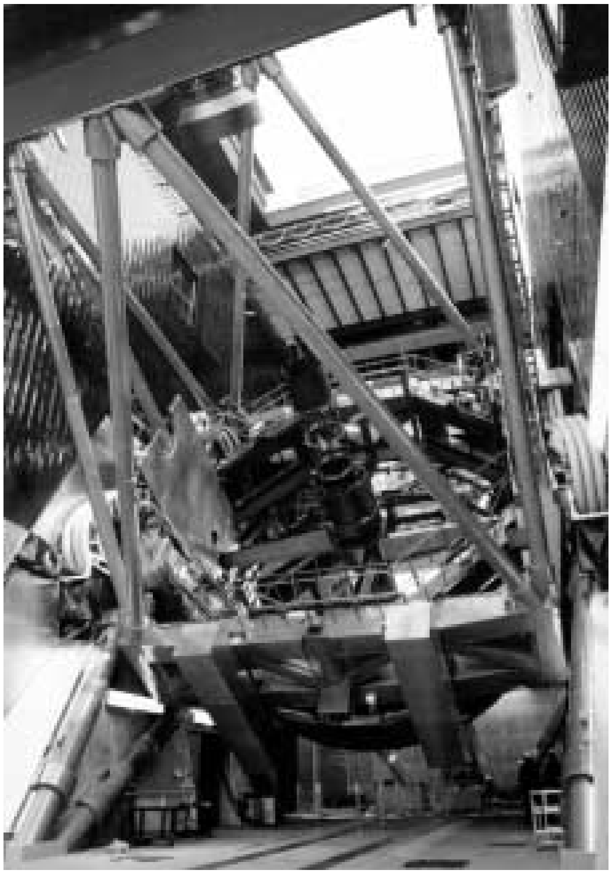

Fig. 2: Main structure of the Subaru telescope in the enclosure.

camera CISCO (Cooled Infrared Spectrograph and Camera for OHS) equipped with a 1 K×1 K HgCdTe detector. The new infrared image reveals fine and faint details of the BN/KL region (upper middle), the bright bar (lower left), and other conspicuous features.

The molecular hydrogen emission around Orion BN/KL is shown in Figure 4. Numerous limb-brightened “finger” features are seen emanating from the patchy central region. Comparison of the image with the one obtained with the *Hubble Space Telescope* (Schultz et al. 1999) shows that the Subaru telescope has a higher sensitivity than the HST with a comparable resolution in the near-infrared. Several finger features pointing toward the north are as long as $100''$ (0.23 pc). Long finger features are also seen in the eastern part where the extinction is higher than that on the other side. The entire H_2 emission resembles a butterfly with its wings spread. This appearance is due to the narrow region of high extinction toward the activity center (IRc 2 or the radio source I). The intrinsic H_2 emission may be more isotropic than it appears to be.

There are 516 point sources detected in the K'-band without being saturated. The luminosity function of these sources has a peak at $K' \sim 12$ mag with a long tail down to $K' \sim 17$ mag. Several tens of these sources are fainter than the hydrogen burning limit of 0.08 $M_\odot$ at their assumed age of 1 $M_{\rm yr}$ and may be young brown dwarfs.

Table 1: Subaru Telescope Overview

Owner	National Astronomical Observatory of Japan (Inter-university research institute)
Construction	1991 – 1999 (9 years)
Total Budget	US$ 360 M
Open Use	Starting from 2000
Total Weight	500 t
Mounting	Altitude-azimuth
Tracking Accuracy	$0''.07$ rms
Primary Mirror Diameter	8.2 m effective / 8.3 m physical
Primary Mirror Material	ULE (ultra-low thermal expansion glass)
Primary Mirror Figure	Thin meniscus supported by 261 actuators
Primary Mirror Focal Length	15 m
Wavelength	0.35 μm – 30 μm
Angular Resolution	$0''.2$ – $0''.5$ ($\sim$50% at K) $0''.3$ – $0''.6$ ($\sim$50% at R) ($0''.05$ expected with AO at K)
Focal Ratio	12.2 (Cassegrain), 12.6 (Nasmyth), and 2.0 (Prime)
Field of View	$6'$ (Cassegrain and Nasmyth) and $30'$ (Prime)

Table 2: Observing Instruments

IRCS (AO)	Infrared Camera and Spectrograph 1-5 μm camera with a high dispersion (R=20,000) echelle spectrograph
CIAO (AO)	Coronagraphic Imager with Adaptive Optics 1-5 μm camera with coronagraph
FOCAS	Faint Object Camera And Spectrograph Optical Imager with a multi-slit spectrograph
COMICS	Cooled Mid-Infrared Camera and Spectrograph Mid-infrared imager and spectrograph
OHS/CISCO	OH-airglow Suppression Spectrograph 1-2.4 μm spectrograph with an OH-line suppressor
HDS	High Dispersion Spectrograph Optical high dispersion (R=100,000) spectrograph
Suprime-Cam	Subaru Prime Focus Camera Optical wide field ($30'$) imager

2.2 A Pair of Twisted Jets from L 1551 IRS 5

Figure 5 shows a J-band image of two ionized jets ejected from the accreting protostar L 1551 IRS 5 (Itoh et al. 2000). While this object has long been believed to be a single forming star, it has recently been resolved into two sources separated by $\sim 0''.3$ (40 pc). The jets, possibly

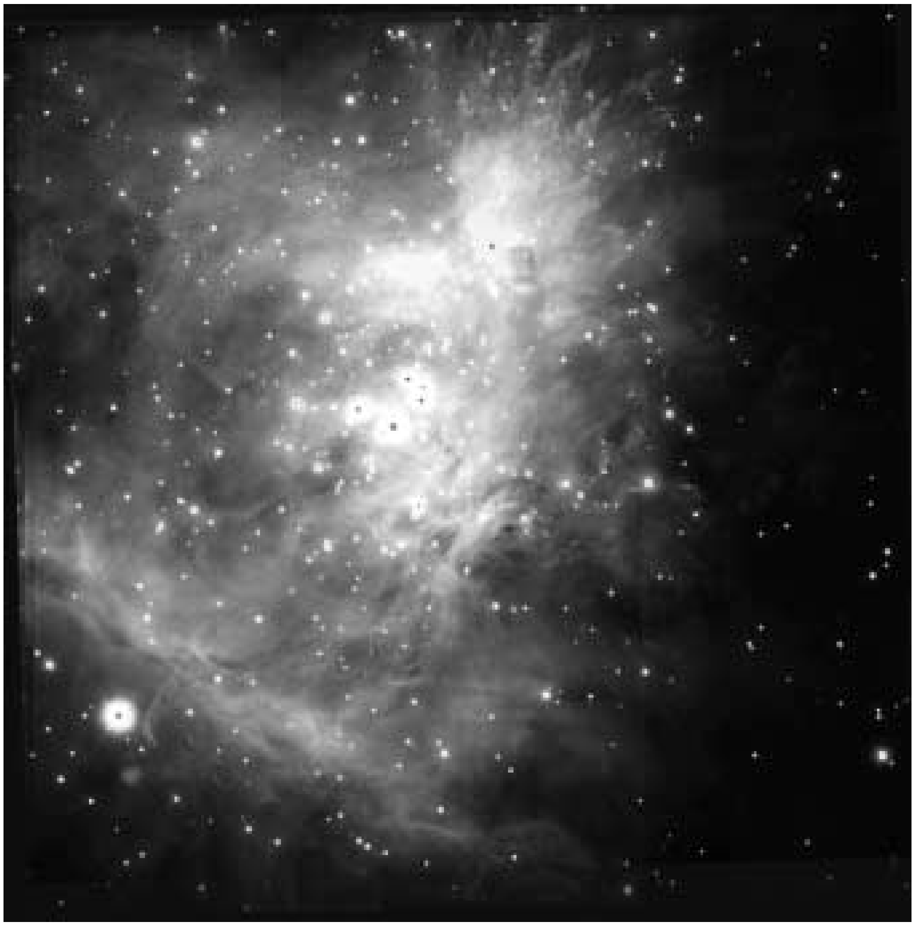

Fig. 3: Composite J, K', and H$_2$ $v = 1 - 0$ S(1) image of the Orion nebula (original in color).

emanating from each of the binary stars, were for the first time resolved into two from the ground, showing a twisted, knotty appearance. Successive grism spectroscopy showed that the jets are bright in [Fe II] lines. The two jets are parallel to each other directing toward west-southwest. The flow direction near the origin is, on the other hand, toward the southwest. Both jets change their directions in a similar way suddenly at $4''$ away from the origin. Comparison with an R-band HST image (Fridlund & Liseau 2000) shows that the jets share the similar knotty appearance and relative brightness distribution between the R and J-bands, suggesting that the twisted and knotty morphology is not due to differential extinction but is intrinsic. The length of the jets are $10''$ (1400 pc), which gives a dynamical time scale of 30 yr with its assumed velocity of 200 kms^{-1}. The short time scale implies that a dynamical effect such as the precession of two jet sources may not be responsible for the twist. The twist might rather be a result of magnetic deflection.

2.3 Gravitational Lens System PG 1115+080

Figure 6 shows the R, J, and K' composite (left) and K'-band (right) images of the gravitational lens system PG 1115+080 (Iwamuro et al. 2000). The J and K' frames were obtained with CISCO, and the R frame was taken with Suprime-Cam equipped with six 2 K×4 K CCDs and

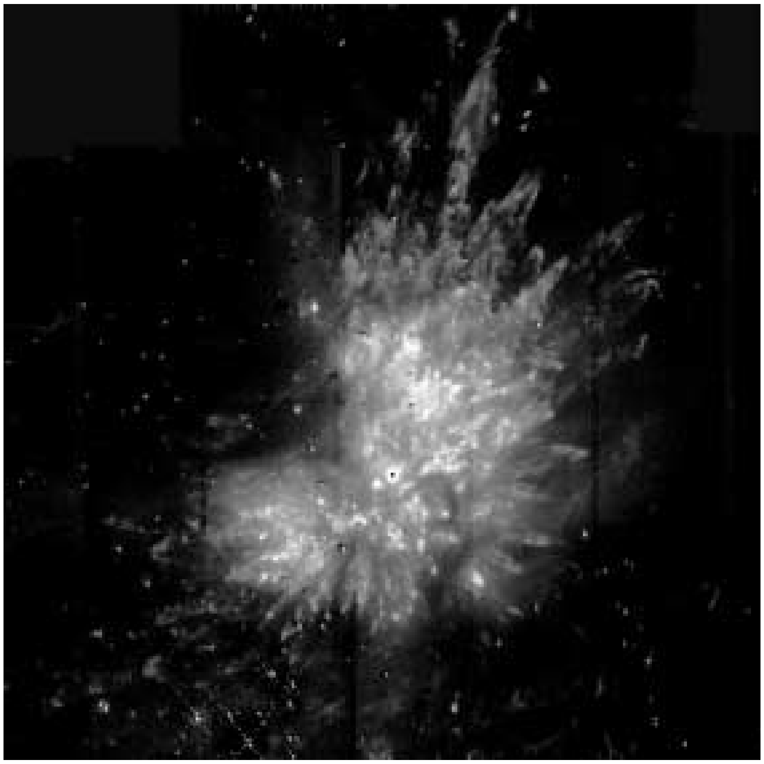

Fig. 4: H_2 $v = 1 - 0$ image of the Orion BN/KL region.

mounted on the Cassegrain focus for the first light program. A lensing galaxy at the center and four lensed quasars surrounding it are well separated from each other, despite their small angular separation of $1''$. The two bright quasar images in the east have weak elongated emission components connecting the two. This emission was first detected with the current observations and suggests that the quasar has a fairly bright emission region with a characteristic size of $\sim$40 pc, which is significantly larger than the size of ordinary broad line regions. Faint extended features at the K'-band are enhanced in the right panel, showing an Einstein ring connecting the four quasar images. The Einstein ring exhibits a significantly red $J - K'$ color compared to a synthetic model galaxy with the age of the universe at the quasar redshift.

3. EXPECTATION FOR THE HII/L2 MISSION SPICA

The HII/L2 mission SPICA mainly targets the mid and far-infrared wavelengths which are more or less in-between the wavelengths to be covered by the similar space missions NGST and FIRST, respectively. The complementary wavelength coverage is important. Considering that mid and far-infrared space missions such as SIRTF, SOFIA, or ASTRO-F are available in the early part of this decade, I believe that the most important characteristics of SPICA is its high angular resolution. The angular resolution of SPICA is $\sim 1''$ at 30 μm. SPICA will play a major role in detailed observations of specific objects with angular resolutions 3–4 times higher than those of the other mid and far-infrared missions.

The resolution of $1''$ corresponds, for example, to 10–100 AU for the planet forming disks around nearby stars at distances of 10–100 pc. The linear size is comparable to or smaller than

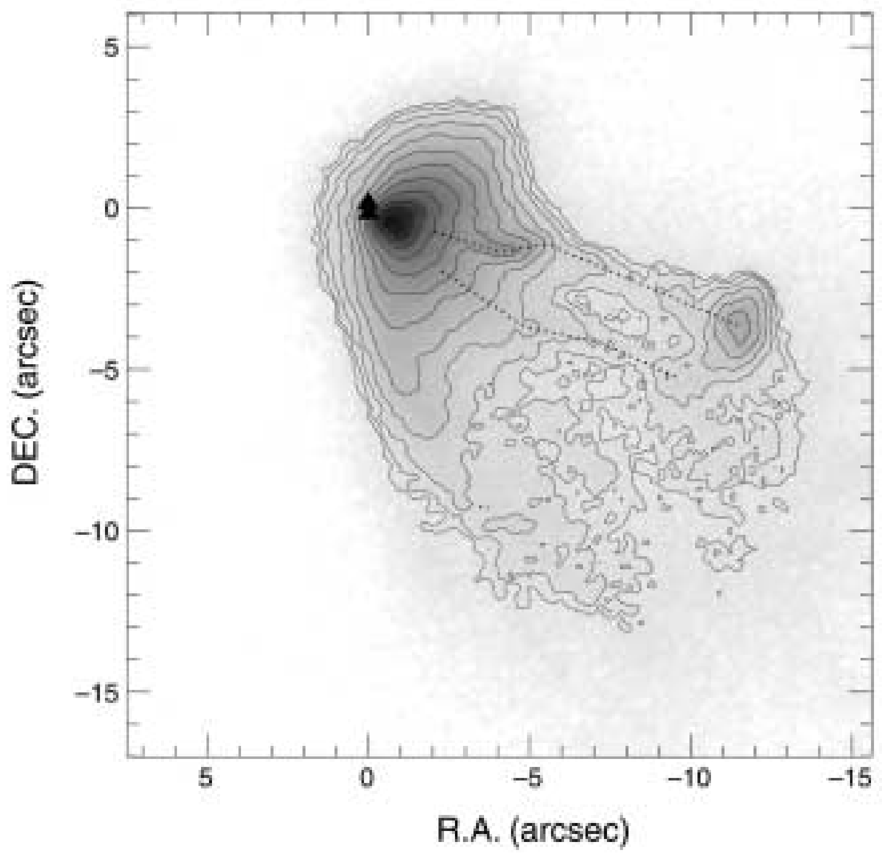

Fig. 5: J-band image of the two jets from L 1551 IRS 5.

the size of protoplanetary disks and will allow us to study their detailed structure in *emission*.

Large ground-based telescopes and HST certainly provide higher angular resolution for such studies. With these telescopes, however, protoplanetary disks have so far been observed in reflection or in silhouette against bright background emission at optical and near-infrared wavelengths. This makes their studies biased toward objects with specific inclinations or regions like Orion nebula, and the number of nearby ($\lesssim$100 pc) objects studied is very limited. SPICA, on the other hand, will directly detect emission from disks without biases, allowing us to make systematic studies of planet forming processes by tracing morphological changes of disks with time.

SPICA will play roles complementary to large submillimeter interferometers such as ALMA/ LMSA, which are planned to start operations within this decade. Although these interferometers provide much higher resolutions of $0.''01$-$0.''1$ than SPICA, their sensitivities are 0.1–1 mJy at the wavelength of $\sim$500 μm. SPICA has a sensitivity better than 0.01 mJy at 30 μm. ALMA/LMSA will resolve, in detail, the structure of nearby protoplanetary disks that have relatively strong dust emission, whereas SPICA will detect much fainter sources and resolve disk structure at a moderate resolution.

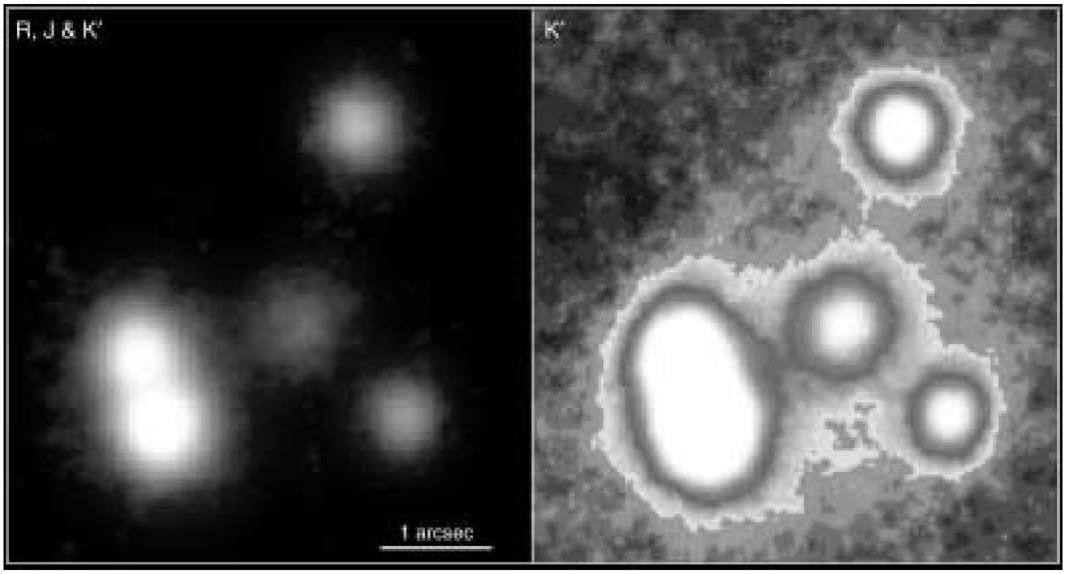

Fig. 6: (Left) Composite R, J, and K' image of the Gravitational lens system PG 1115+080. (Right) K'-band image with faint extended features enhanced.

ACKNOWLEDGMENT

Please refer to `http://subarutelescope.org/` to find original color images of the gray scale pictures used in this article.

REFERENCES

Kaifu, N., et al., 2000, PASJ, 52, 1
Iwamuro, F. et al. 2000, PASJ, 52, 25
Itoh, Y. et al. 2000, PASJ, 52, 81
Fridlund, C. V. M., & Liseau, R. 2000, ApJ, 499, L75
Schultz, A. S. B. et al. 1999, ApJ, 511, 282